CHAPTER 4.

Moisture Deficit and Surplus in the Conterminous United States for Three Time Windows: 2016, 2014–2016, and 2012–2016

FRANK H. KOCH

JOHN W. COULSTON

INTRODUCTION

Droughts affect most forested ecosystems of the United States, but they vary widely in frequency and intensity (Hanson and Weltzin 2000). Most western U.S. forests experience annual seasonal droughts, with the seasonality determined by broad-scale atmospheric circulation patterns and topography. For example, forests along the Pacific Coast usually experience dry summers and wet winters, while forests in Arizona and western New Mexico rely in part on rainfall received during a summer monsoon season (Adams and Comrie 1997, Hanson and Weltzin 2000). In contrast, eastern U.S. forests typically exhibit one of two predominant drought patterns: random (i.e., occurring at any time of year) occasional droughts, as observed in the Appalachian Mountains and the Northeast, or frequent late-summer droughts, as commonly seen in the southeastern Coastal Plain and the eastern portion of the Great Plains (Hanson and Weltzin 2000).

In forests, reduced moisture availability during droughts can cause considerable tree stress, and that stress is amplified when droughts coincide with hot conditions, especially heat waves or other extreme heat events (Allen and others 2010, L.D.L. Anderegg and others 2013, Peters and others 2015, Teskey and others 2015, Williams and others 2013). Trees, like other plants, respond initially to drought stress by decreasing fundamental growth processes such as cell division and enlargement. Because photosynthesis is less sensitive than these fundamental processes, it decreases slowly at low levels of stress. However, as drought stress intensifies, trees and other plants close their stomata to minimize water loss, causing photosynthesis to decline more sharply (Kareiva and others 1993, Kolb and others 2016, Mattson and Haack 1987). In addition to such direct effects, drought stress often makes trees susceptible to attack by damaging insects and diseases (Clinton and others 1993, Mattson and Haack 1987, Raffa and others 2008), although this may be more of a problem in the water-limited forests of the Western United States (Kolb and others 2016). Droughts also increase wildland fire risk by inhibiting organic matter decomposition and lowering the moisture content of downed woody debris and other potential fire fuels (Clark 1989, Keetch and Byram 1968, Schoennagel and others 2004, Trouet and others 2010).

In general, forests are resistant to short-term droughts, although individual tree species differ in their levels of drought resistance (Archaux and Wolters 2006, Berdanier and Clark 2016). Because of this resistance, the duration of drought events may be more important for forests than their intensity (Archaux and Wolters 2006). For instance, forested areas subjected to multiple consecutive years of drought (2–5 years) are much more likely to experience high tree mortality than areas subjected to a single year of extremely dry conditions (Guarín and Taylor 2005, Millar and others 2007). Therefore, a comprehensive evaluation of drought impact in forests should include analysis of moisture conditions over multi-year time windows.

In the 2010 Forest Health Monitoring (FHM) national report, we described a method for mapping drought conditions across the conterminous United States (Koch and others 2013a). Our objective was to generate fine-scale, drought-related spatial datasets that improve upon similar products available from sources such as the National Climatic Data Center (2015) or the U.S. Drought Monitor program (Svoboda and others 2002). The principal inputs are gridded climate data (i.e., monthly raster maps of precipitation and temperature over a 100-year period) created with the Parameter-elevation Regression on Independent Slopes (PRISM) climate mapping system (Daly and others 2002). The method utilizes a standardized indexing approach that facilitates comparison of a given location's moisture status during different time windows, regardless of their length. The index is easier to calculate than the commonly used Palmer Drought Severity Index, or PDSI (Palmer 1965), and avoids some criticisms of the PDSI (summarized by Alley 1984) regarding its underlying assumptions and limited comparability across space and time. Here, we applied the method outlined in the 2010 FHM Report to the most currently available climate data (i.e., the monthly PRISM data through 2016), thereby providing the eighth installment in an ongoing series of annual drought assessments for the conterminous United States from 2009 forward (Koch and Coulston 2015, 2016, 2017; Koch and others 2013a, 2013b, 2014, 2015).

This is the third year in which we also mapped the degree of moisture surplus across the conterminous United States during multiple time windows. Much recent refereed literature (e.g., Adams and others 2009, Allen and others 2010, Martínez-Vilalta and others 2012, Peng and others 2011, Williams and others 2013) has tended to focus on reports of widespread, regional-scale forest decline and mortality due to persistent drought conditions, especially in conjunction with periods of extremely high temperatures (i.e., heat waves). However, surplus moisture availability can also be detrimental to forests. Abnormally high moisture can be a short-term stressor (e.g., an extreme rainfall event with subsequent flooding) or a long-term stressor (e.g., persistent wetness driven by a macroscale climatic pattern such as the El Niño-Southern Oscillation), either of which may contribute to tree dieback and mortality (Rozas and García-González 2012, Rozas and Sampedro 2013). Such impacts have been observed in both tropical and temperate forests (Laurance and others 2009, Rozas and García-González 2012). While surplus-induced impacts in forests are probably not as common as drought-induced impacts, a single index that depicts both moisture surplus and deficit conditions provides a fuller accounting of potential forest health issues.

METHODS

We acquired grids for monthly precipitation and monthly mean temperature for the conterminous United States from the PRISM Climate Group Web site (PRISM Climate Group 2017). At the time of these analyses, gridded datasets were available for all years from 1895 to 2016. However, the grids for December 2016 were only provisional versions (i.e., finalized grids had not yet been released). For analytical purposes, we treated these provisional grids as if they were the final versions. The spatial resolution of the grids was approximately 4 km (cell area = 16 km^2). For future applications and to ensure better compatibility with other spatial datasets, all output grids were resampled to a spatial resolution of approximately 2 km (cell area = 4 km^2) using a nearest neighbor approach. The nearest neighbor approach is a computationally simple resampling method that avoids the smoothing of data values observed with methods such as bilinear interpolation or cubic convolution.

Potential Evapotranspiration (PET) Maps

As in our previous drought mapping efforts (Koch and Coulston 2015, 2016, 2017; Koch and others 2012a, 2012b, 2013a, 2013b, 2014, 2015), we adopted an approach in which a moisture index value is calculated for each location of interest (i.e., each grid cell in a map of the conterminous United States) during a given time period. Moisture indices are intended to reflect the amount of available water (e.g., to support plant growth) in different locations. By extension, they also depict the relative wetness or dryness of those locations (Willmott and Feddema 1992). Generally, moisture indices are computed as functions of the ratio of moisture supply to moisture demand (Willmott and Feddema 1992). In our case, the index is computed as a function of the amount of precipitation that falls on a location during the time period of interest (i.e., the moisture supply) as well as the level of potential evapotranspiration during this period (i.e., the moisture demand). Potential evapotranspiration measures the loss of soil moisture through plant uptake and transpiration (Akin 1991). It does not measure actual moisture loss, but rather the loss that would occur if there was no possible shortage of moisture for plants to transpire (Akin 1991, Thornthwaite 1948).

To complement the available PRISM monthly precipitation grids, we computed corresponding monthly potential evapotranspiration (*PET*) grids using Thornthwaite's formula (Akin 1991, Thornthwaite 1948):

$$PET_m = 1.6L_{lm}(10\frac{T_m}{I})^a \qquad (1)$$

where

PET_m = the potential evapotranspiration for a given month *m* in cm

L_{lm} = a correction factor for the mean possible duration of sunlight during month *m* for all locations (i.e., grid cells) at a particular latitude *l* [see table V in Thornthwaite (1948) for a list of *L* correction factors by month and latitude]

T_m = the mean temperature for month *m* in degrees C

I = an annual heat index, calculated as

$$I = \sum_{m=1}^{12} \left(\frac{T_m}{5}\right)^{1.514}$$

where

T_m is the mean temperature for each month *m* of the year

a = an exponent calculated as $a = 6.75 \times 10^{-7} I^3 - 7.71 \times 10^{-5} I^2 + 1.792 \times 10^{-2} I + 0.49239$ [see appendix I in Thornthwaite (1948) regarding calculation of *I* and the empirical derivation of *a*]

Although only a simple approximation, a key advantage of Thornthwaite's formula is that it has modest input data requirements (i.e., mean temperature values) compared to more sophisticated methods of estimating PET such as the Penman-Monteith equation (Monteith 1965), which requires less readily available data on factors such as humidity, radiation, and wind speed. To implement Equation 1 spatially, we created a grid of latitude values for determining the *L* adjustment for any given grid cell (and any given month) in the conterminous United States. We extracted the T_m values for the grid cells from the corresponding PRISM mean monthly temperature grids.

Moisture Index Maps

To estimate baseline conditions, we used the precipitation (*P*) and *PET* grids to generate moisture index grids for the past 100 years (i.e., 1917-2016) for the conterminous United States. We used a moisture index described by Willmott and Feddema (1992), which has been applied in a variety of contexts, including global vegetation modeling (Potter and Klooster 1999) and climate change analysis (Grundstein 2009). Willmott and Feddema (1992) devised the index as a refinement of one described earlier by Thornthwaite (1948) and Thornthwaite and Mather (1955). Their revised index, *MI'*, has the following form:

$$MI' = \begin{cases} P/PET - 1 & , \quad P < PET \\ 1 - PET/P & , \quad P \geq PET \\ 0 & , \quad P = PET = 0 \end{cases} \qquad (2)$$

where

P = precipitation

PET = potential evapotranspiration, as calculated using Equation 1

(P and PET must be in equivalent measurement units, e.g., mm)

This set of equations yields an index that varies between -1 and 1, with negative values indicating dry conditions and positive values indicating wet conditions. In addition, MI' is symmetric about zero. A primary advantage of this symmetry is that it enables valid comparisons between any set of locations in terms of their moisture balance (i.e., the balance between moisture demand and supply). Willmott and Feddema (1992) illustrated the index with examples where they calculated MI' values on an annual basis (i.e., using total P and PET values summed across one calendar year). In fact, MI' can be calculated for any time period using this summation approach, although the resulting values may be biased if calculated for periods of less than a year (Willmott and Feddema 1992). An alternative to summation is to calculate MI' separately for each month in a time window of interest, and then compute the mean of the MI' values for all months in the time window. This "mean-of-months" approach limits the ability of short-term peaks in either precipitation or potential evapotranspiration to negate corresponding short-term deficits, as would happen under a summation approach.

For each year in our study period (i.e., 1917-2016), we used the mean-of-months approach to calculate moisture index grids for three different time windows: 1 year (MI_1'), 3 years (MI_3'), and 5 years (MI_5'). Briefly, the MI_1' grids are the mean (i.e., the mean value for each grid cell) of the 12 monthly MI' grids for each year in the study period, the MI_3' grids are the mean of the 36 monthly grids from January of 2 years prior through December of the target year, and the MI_5' grids are the mean of the 60 consecutive monthly MI' grids from January of 4 years prior to December of the target year. Thus, the MI_1' grid for the year 2016 is the mean of the monthly MI' grids from January to December 2016, while the MI_3' grid is the mean of the grids from January 2014 to December 2016, and the MI_5' grid is the mean of the grids from January 2012 to December 2016.

Annual and Multi-Year Drought Maps

To determine degree of departure from typical moisture conditions, we first created a normal grid, $MI_i'{}_{norm}$, for each of our three time windows, representing the mean (i.e., the mean value for each grid cell) of the 100 corresponding moisture index grids (i.e., the MI_1', MI_3', or MI_5' grids, depending on the window; see fig. 4.1). We also created a standard deviation grid, $MI_i'{}_{SD}$, for each time window, calculated from the window's 100 individual moisture index grids as well as its $MI_i'{}_{norm}$ grid.

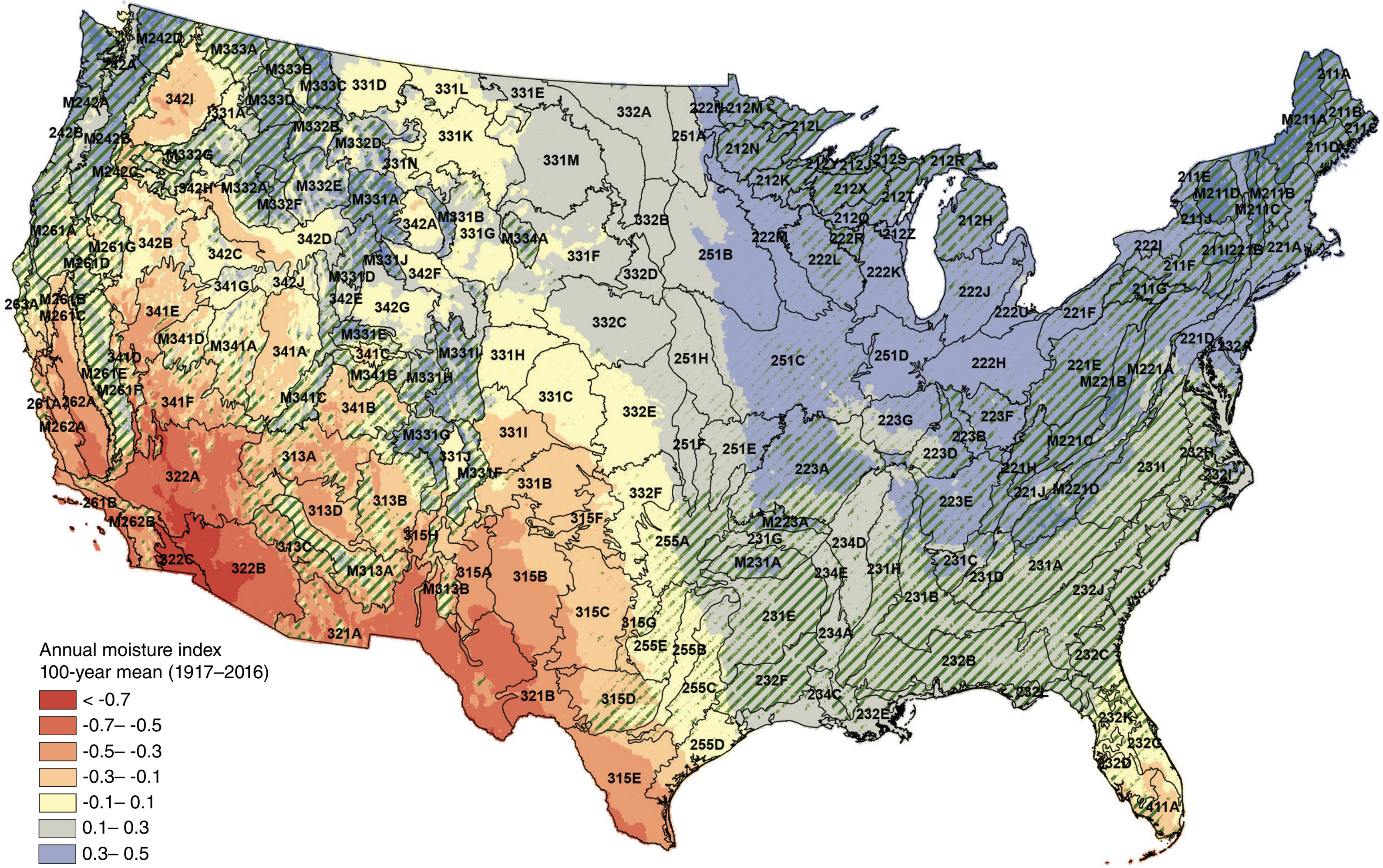

Figure 4.1—The 100-year (1917–2016) mean annual moisture index, or $MI_{1'norm}'$*, for the conterminous United States. Ecoregion section (Cleland and others 2007) boundaries and labels are included for reference. Forest cover data (overlaid green hatching) derived from Moderate Resolution Imaging Spectroradiometer (MODIS) imagery by the U.S. Department of Agriculture, Forest Service, Remote Sensing Applications Center. (Data source: PRISM Climate Group, Oregon State University)*

We subsequently calculated moisture difference z-scores, MDZ_{ij}, for each time window using these derived datasets:

$$MDZ_{ij} = \frac{MI_i' - MI_i'_{norm}}{MI_i'_{SD}} \qquad (3)$$

where

i = the analytical time window (i.e., 1, 3, or 5 years) and

j = a particular target year in our 100-year study period (i.e., 1917-2016).

MDZ scores may be classified in terms of degree of moisture deficit or surplus (table 4.1). The classification scheme includes categories (e.g., severe drought, extreme drought) like those associated with the PDSI. The scheme has also been adopted for other drought indices such as the Standardized Precipitation Index, or SPI (McKee and others 1993). Moreover, the breakpoints between *MDZ* categories resemble those used for the SPI, such that we expect the *MDZ* categories to have theoretical frequencies of occurrence that are similar to their SPI counterparts (e.g., approximately 2.3 percent of the time for extreme drought; see McKee and others 1993, Steinemann 2003). More importantly, because of the standardization in Equation 3, the breakpoints between categories remain the same regardless of the size of the time window of interest. For comparative analysis, we generated and classified *MDZ* maps of the conterminous United States, based on all three time windows, for the target year 2016.

Table 4.1—Moisture difference *z*-score (*MDZ*) value ranges for nine wetness and drought categories, along with each category's approximate theoretical frequency of occurrence

MDZ Score	Category	Frequency
< -2	Extreme drought	2.3%
-2 to -1.5	Severe drought	4.4%
-1.5 to -1	Moderate drought	9.2%
-1 to -0.5	Mild drought	15.0%
-0.5 to 0.5	Near normal conditions	38.2%
0.5 to 1	Mild moisture surplus	15.0%
1 to 1.5	Moderate moisture surplus	9.2%
1.5 to 2	Severe moisture surplus	4.4%
> 2	Extreme moisture surplus	2.3%

RESULTS AND DISCUSSION

The 100-year (1917–2016) mean annual moisture index, or $MI_1'_{norm}$, grid (fig. 4.1) serves as an overview of climatic regimes in the conterminous United States. (The 100-year $MI_3'_{norm}$ and $MI_5'_{norm}$ grids were similar to the $MI_1'_{norm}$ grid, and so are not shown here.) Wet climates ($MI' > 0$) are common in the Eastern United States, particularly the Northeast. A noteworthy anomaly is southern Florida, especially ecoregion sections (Cleland and others 2007) 232D–Florida Coastal Lowlands-Gulf, 232G–Florida Coastal Lowlands-Atlantic, and 411A–Everglades, which appear to be dry relative to other parts of the East. This is an effect of the region's tropical climate, which has distinct wet (primarily summer months) and dry (late fall to early spring) seasons. Although southern Florida usually receives a high level of precipitation during the wet season, it can be insufficient to offset the region's lengthy dry season (Duever and others 1994) or its high level of evapotranspiration, especially during the late spring and summer months, resulting in negative *MI'* values.

The comparatively dry climatic regime of southern Florida is markedly different from the extremely dry regimes seen in parts of the Western United States, especially the Southwest (e.g., sections 322A–Mojave Desert, 322B–Sonoran Desert, and 322C–Colorado Desert), where potential evapotranspiration is very high, but precipitation levels are very low. Indeed, dry climates ($MI' < 0$) are typical across much of the Western United States because of generally lower precipitation than the East. Nevertheless, mountainous areas in the central and northern Rocky Mountains as well as the Pacific Northwest are relatively wet, such as ecoregion sections M242A–Oregon and Washington Coast Ranges, M242B–Western Cascades, M331G–South Central Highlands, and M333C–Northern Rockies. This is driven in part by large amounts of winter snowfall in these regions (Hanson and Weltzin 2000).

Figure 4.2 shows the annual (i.e., 1-year) *MDZ* map for 2016 for the conterminous United States. Perhaps the most notable feature of the map is a large area of severe to extreme drought ($MDZ < -1.5$) extending across much of the Southeastern United States, especially sections 221H–Northern Cumberland Plateau, 221J–Central Ridge and Valley, 231A–Southern Appalachian Piedmont, 231C–Southern Cumberland Plateau, and 231D–Southern Ridge and Valley; the southern portion of M221D–Blue Ridge Mountains; and the southwestern portion of 231I–Central Appalachian Piedmont. This area of drought developed primarily in the latter half of 2016, and expanded to occupy nearly 55 percent of the Southeast at the end of November, according to the U.S. Drought Monitor (National Climatic Data Center 2017b). During fall 2016, many locations throughout the region went more than 50 consecutive days without precipitation (National Climatic Data Center 2017b). These dry conditions have been cited as one of the main factors contributing to an unusually active fall wildfire season in the Southeastern United States, especially in the Southern Appalachian Mountains: by the end of 2016, 50 major fires had burned close to 100,000 acres in this subregion alone (Boddy 2016, Southeast Regional Climate Center 2016). However, unusually warm temperatures also played a significant role in promoting wildfire activity. In terms of average monthly temperatures, 2016 was the warmest year on record for the Southeast; in the Southern Appalachian Mountains specifically, average maximum temperatures during the July–December 2016 period were as much as 2.5 ^{o}C higher than the 20th-century averages for this period (National Climatic Data Center 2017a). Additionally, local weather conditions (e.g., high winds) facilitated the rapid expansion of some fires, thereby increasing their geographic footprints and subsequent impacts on the landscape.

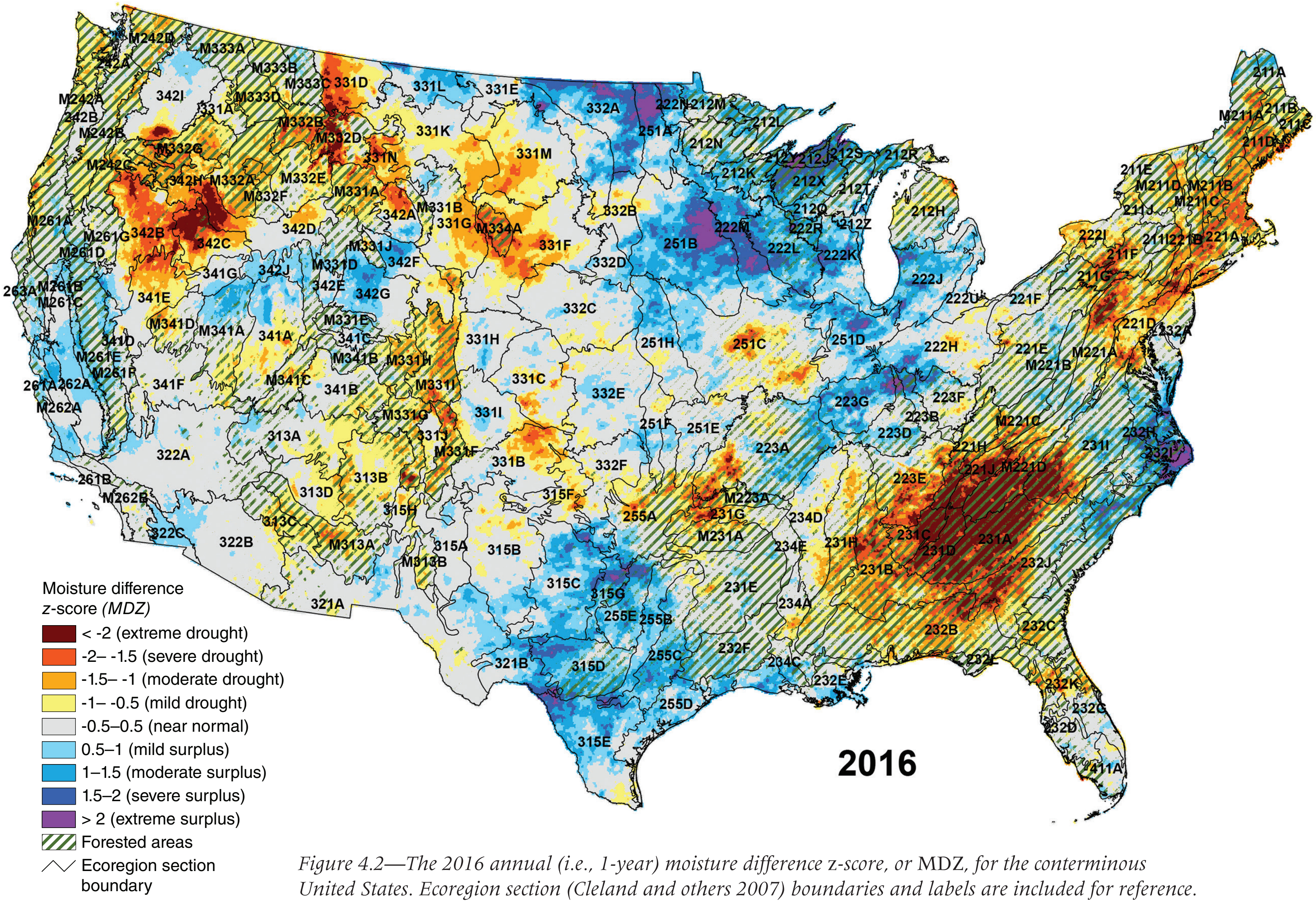

Figure 4.2—The 2016 annual (i.e., 1-year) moisture difference z-score, or MDZ, for the conterminous United States. Ecoregion section (Cleland and others 2007) boundaries and labels are included for reference. Forest cover data (overlaid green hatching) derived from MODIS imagery by the U.S. Department of Agriculture, Forest Service, Remote Sensing Applications Center. (Data source: PRISM Climate Group, Oregon State University)

Elsewhere in the Eastern United States, a contiguous area of mostly moderate to extreme drought (*MDZ* < -1) conditions extended north from the Mid-Atlantic region into New England during 2016. Among the most affected ecoregion sections were 211F–Northern Glaciated Allegheny Plateau, 211G–Northern Unglaciated Allegheny Plateau, 221A–Lower New England, and the northern portion of M221A–Northern Ridge and Valley (northern portion); much of Maine (sections M211A–White Mountains and 211D–Central Maine Coastal and Embayment) also experienced moderate to severe drought conditions. In some locations within this area, drought conditions reached historical extremes during 2016. For example, as measured by PDSI, 2016 was the driest year on record for the Connecticut coast and the second driest year on record for Long Island in New York (National Climatic Data Center 2017a).

The 2016 *MDZ* map (fig. 4.2) shows two other areas of severe to extreme drought in the northwestern portion of the United States. The larger of these, in eastern Oregon and southwestern Idaho, occurred primarily in sections 342B–Northwestern Basin and Range, 342C–Owyhee Uplands, and 342D–Snake River Basalts and Basins, all of which have little forest. The second area covered much of western Montana, but extreme drought conditions were mostly limited to section M332D–Belt Mountains. Scattered areas of moderate to extreme drought appeared elsewhere in the Western and Central United States. One such area was centered on forested section M334A–Black Hills and extended into neighboring sections with little or no forest (e.g., 331F–Western Great Plains and 331M–Missouri Plateau). Another area extended across portions of sections 223A–Ozark Highlands, M223A–Boston Mountains, 231G–Arkansas Valley, and M231A–Ouachita Mountains. Moderate to extreme drought conditions also affected the Front Range of the Rocky Mountains in Colorado and northern New Mexico (sections M331F–Southern Parks and Rocky Mountain Range and M331I–Northern Parks and Ranges).

Drought conditions were conspicuously absent throughout most of California during 2016. As measured by PDSI, 2016 was only the 35th driest year in the State's history, and the wettest year since 2011 (National Climatic Data Center 2017a). This is in stark contrast to 2015 (fig. 4.3), when almost all of the forested areas in California experienced severe to extreme drought conditions. Drought conditions were also much worse in the Pacific Northwest region in 2015 than in 2016. Significantly, temperature was probably the main driver of these conditions: 2015 was the warmest year on record for the Pacific Northwest, and the high temperatures increased evapotranspiration more than enough to offset the region's relatively normal precipitation levels during 2015 (National Climatic Data Center 2017a). By comparison, 2016 was only the sixth warmest year for the region, while precipitation levels were again close to normal. Regardless, these recent circumstances in the Pacific Northwest emphasize the fact that high temperatures

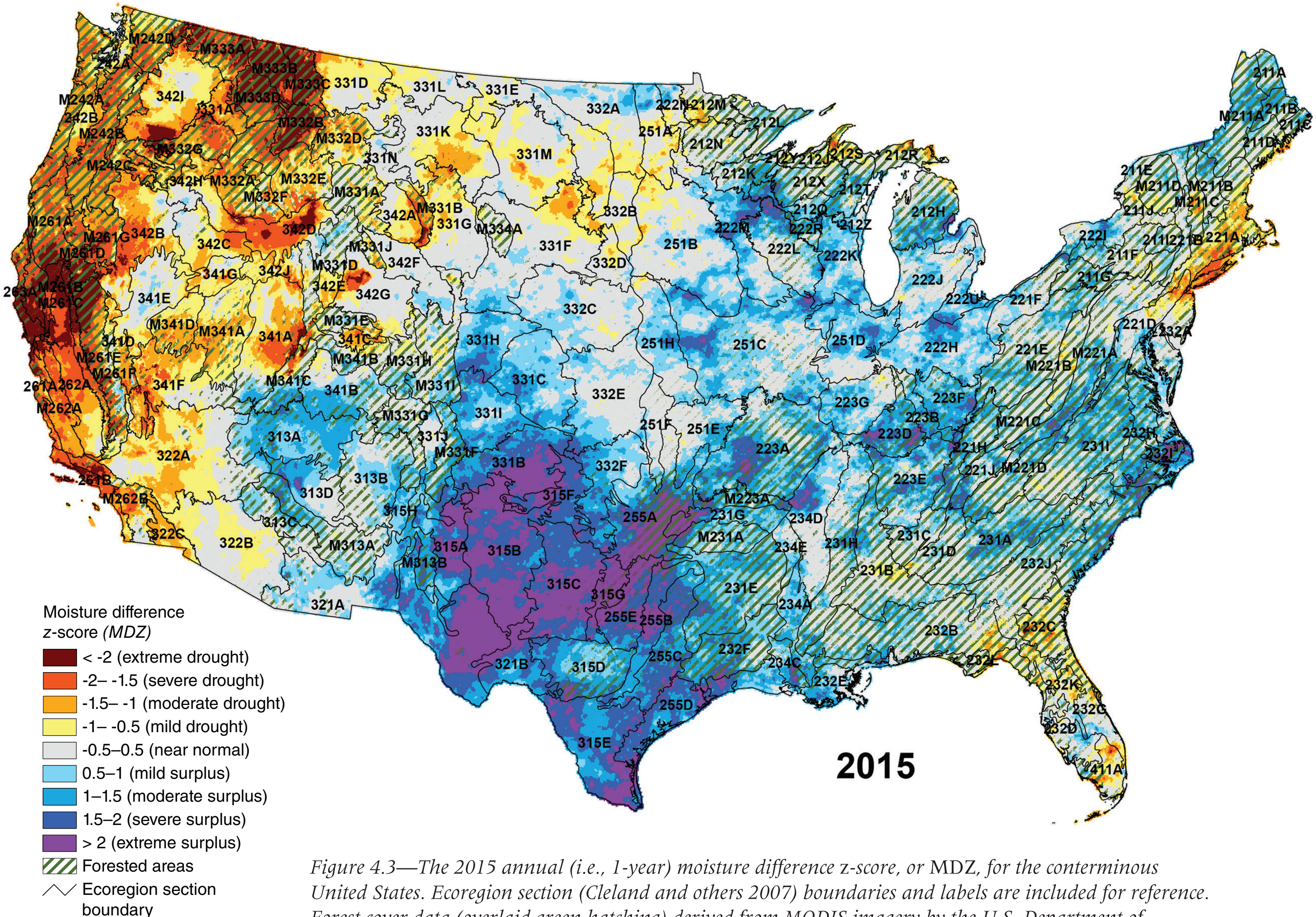

Figure 4.3—The 2015 annual (i.e., 1-year) moisture difference z-score, or MDZ, for the conterminous United States. Ecoregion section (Cleland and others 2007) boundaries and labels are included for reference. Forest cover data (overlaid green hatching) derived from MODIS imagery by the U.S. Department of Agriculture, Forest Service, Remote Sensing Applications Center. (Data source: PRISM Climate Group, Oregon State University)

(i.e., high evapotranspiration) can exacerbate moisture deficits, and in some cases overcome moisture surpluses, thereby increasing drought severity above what might otherwise be expected (Rind and others 1990). This may be especially worrisome given the continued warming trend that has been observed globally due to anthropogenic climate change (Luce and others 2016, Rind and others 1990).

Furthermore, high temperatures can prolong drought-related impacts to forests, including tree mortality, even after moisture availability returns to normal (Mitchell and others 2014), particularly if the preceding drought persisted over multiple years (Berdanier and Clark 2016). This is demonstrated by the massive-scale forest mortality that has occurred in California during the last decade. In November 2016, the Forest Service, U.S. Department of Agriculture, reported that more than 102 million trees have been killed in the State since 2010 due to primary or secondary effects (e.g., bark beetle outbreaks) of drought and extreme heat, with millions more trees expected to die in the near future (USDA Office of Communications 2016). Although California was comparatively wet during 2016 (see fig. 4.2), this came after a period of historically extreme drought conditions that lasted at least 5 years (USDA Office of Communications 2016). More to the point, temperatures remained high in California in 2016: it was the State's third warmest year on record, behind only 2014 and 2015, which were the first and second warmest years, respectively, in terms of both average and maximum temperatures (National Climatic Data Center 2017a).

The California example also reiterates the importance of using longer time windows when assessing potential drought impacts to trees and forests. When considered as forecasts of where such impacts are most likely to emerge, the 3-year (2014–2016; fig. 4.4) and, especially, the 5-year (2012–2016; fig. 4.5) *MDZ* maps for the conterminous United States clearly show significant risk of drought impacts to forests not just in California, but throughout much of the Western United States. In contrast, the 3- and 5-year maps suggest that very few areas in the Central and Eastern United States face a similar degree of drought-related risk. For instance, the 5-year *MDZ* map shows hot spots of moderate to extreme drought in central and southern Florida (sections 232C–Atlantic Coastal Flatwoods, 232D, 232K–Florida Coastal Plains and Central Highlands, and 411A), but the 3-year *MDZ* map indicates that moisture conditions have improved in these areas in the last few years. It is also evident from the multi-year maps – especially when viewed in combination with the 1-year *MDZ* maps for 2015 (fig. 4.3) and 2016 (fig. 4.2) – that drought conditions in the Southern Appalachian Mountains did not begin to emerge until 2016. The one noteworthy case of persistent and intense drought conditions in the East is the previously highlighted area in southern New England and Long Island. In its 2016 annual summary report on drought

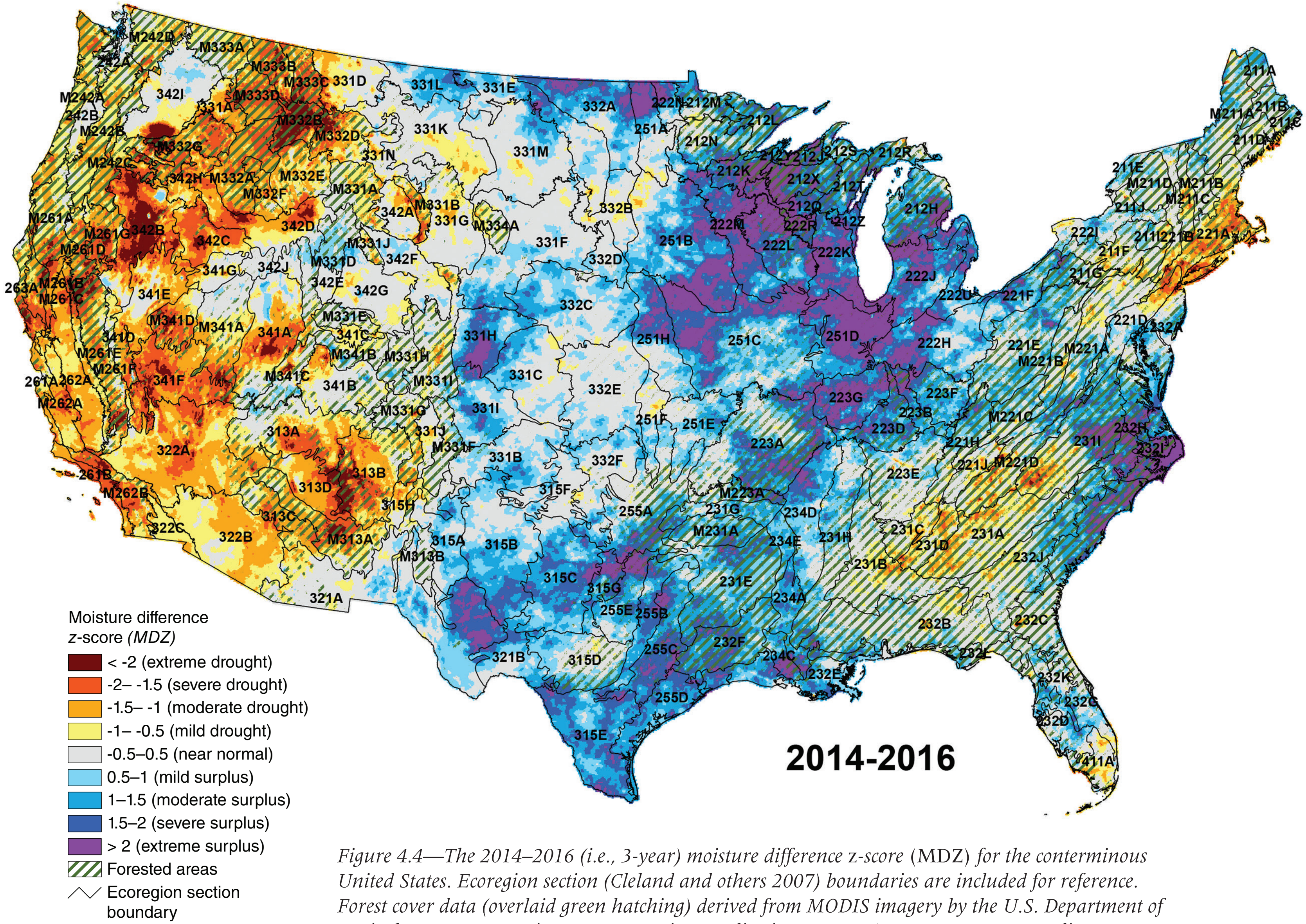

Figure 4.4—The 2014–2016 (i.e., 3-year) moisture difference z-score (MDZ) *for the conterminous United States. Ecoregion section (Cleland and others 2007) boundaries are included for reference. Forest cover data (overlaid green hatching) derived from MODIS imagery by the U.S. Department of Agriculture, Forest Service, Remote Sensing Applications Center. (Data source: PRISM Climate Group, Oregon State University)*

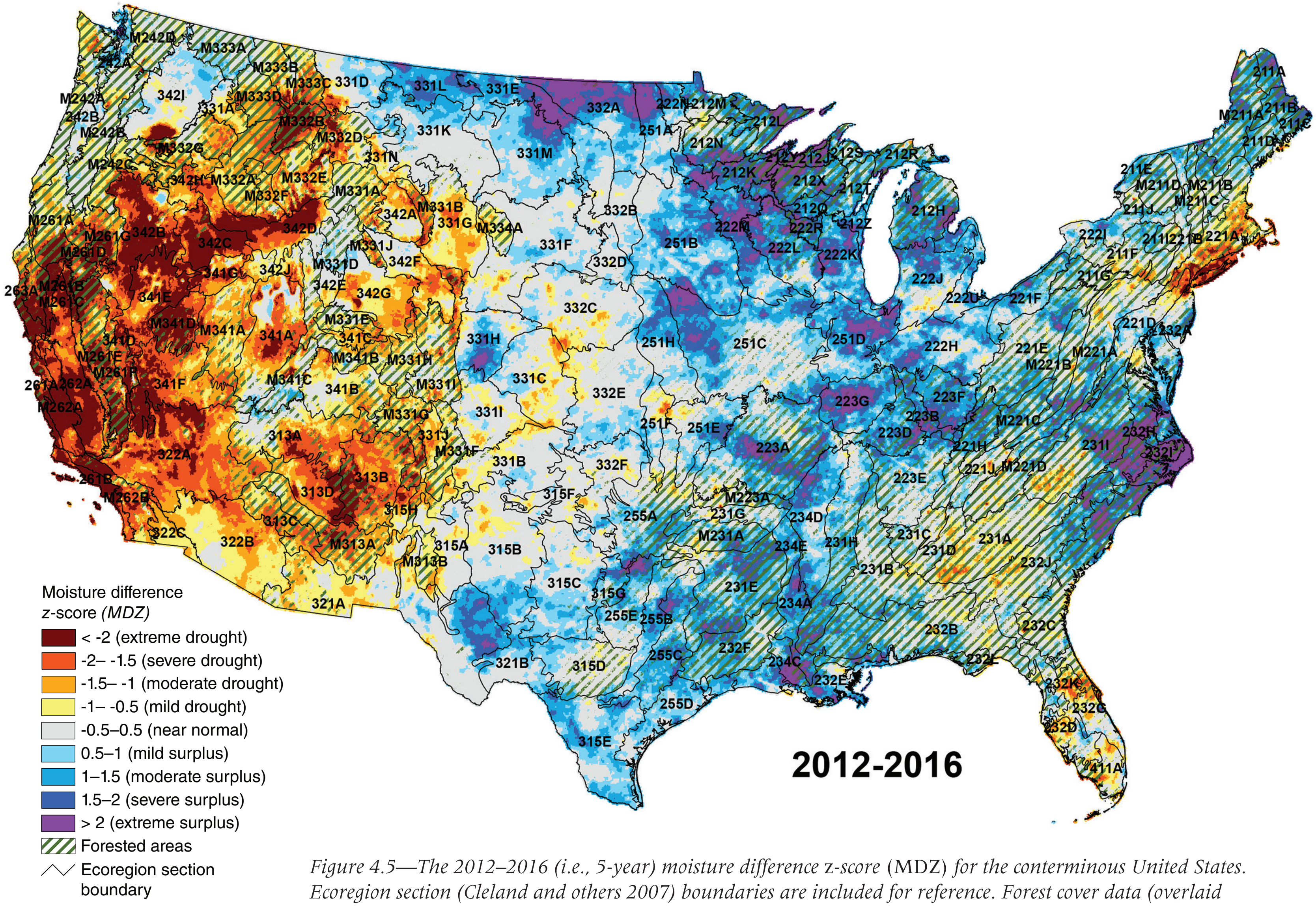

Figure 4.5—The 2012–2016 (i.e., 5-year) moisture difference z-score (MDZ) *for the conterminous United States. Ecoregion section (Cleland and others 2007) boundaries are included for reference. Forest cover data (overlaid green hatching) derived from MODIS imagery by the U.S. Department of Agriculture, Forest Service, Remote Sensing Applications Center. (Data source: PRISM Climate Group, Oregon State University)*

(National Climatic Data Center 2017b), the National Climatic Data Center compared the recent conditions in this area to a historically severe drought that persisted throughout the mid-1960s (documented in Namias 1966, 1983). Data suggest this is an apt comparison; for instance, along the coast of Connecticut, 1962–1966 was the second driest 5-year period on record as measured by PDSI, surpassed only by the 2012–2016 period (National Climatic Data Center 2017a). Although these recent conditions have not been associated with large-scale tree mortality as seen in California, they have been linked to indirect impacts such as defoliation by the European gypsy moth (*Lymantria dispar*) in Connecticut, Rhode Island, and Massachusetts at levels not seen since the 1980s (Elkinton and Boettner 2016).

As with drought, the most relevant moisture surpluses with respect to forest health are probably those that persist for several years. Areas exhibiting severe to extreme surplus conditions in both the 3-year and 5-year *MDZ* maps (figs. 4.4 and 4.5) may merit further attention, since the former would indicate limited recent movement toward more normal moisture conditions. Forested areas exhibiting severe to extreme surpluses over 5 years were distributed widely across the Eastern United States: in North Carolina and South Carolina (portions of 231I–Central Appalachian Piedmont, 232C–Atlantic Coastal Flatwoods, 232H–Middle Atlantic Coastal Plains and Flatwoods, and especially 232I–Northern Atlantic Coastal Flatwoods); in Kentucky (sections 221H–Northern Cumberland Plateau, M221C–Northern Cumberland Mountains, 223B–Interior Low Plateau-Transition Hills, 223D–Interior Low Plateau-Shawnee Hills, and 223F–Interior Low Plateau-Bluegrass); in Arkansas and Louisiana (section 223A–Ozark Highlands and the northern portion of 234D–White and Black River Alluvial Plains); and in Michigan (section 212H–Northern Lower Peninsula). The area of surplus in North and South Carolina is of particular note because of its large size and contiguity, and also because its extent is nearly the same in the 2014–2016 *MDZ* map and the 2012–2016 *MDZ* map. For all Climate Divisions (see Guttman and Quayle 1996) in the eastern portion of both States, 2014–2016 was the wettest 3-year period on record, and 2012–2016 was either the wettest or second wettest 5-year period (National Climatic Data Center 2017a). For example, North Carolina Climate Division 7, which covers the central portion of the State's Coastal Plain, averaged a 3-year precipitation total of 3.87 m during the 20th century, but received 4.72 m of precipitation during the 2014–2016 period. Likewise, this region averaged a 5-year precipitation total of 6.45 m during the 20th century, but received 7.34 m during the 2012–2016 period (National Climatic Data Center 2017a).

Future Efforts

If the appropriate spatial data (i.e., high-resolution maps of precipitation and temperature) remain available for public use, we will continue to produce our 1-year, 3-year, and 5-year *MDZ* maps of the conterminous United States as a regular yearly component of national-scale forest health reporting. However, users should interpret and compare the *MDZ* maps presented here cautiously. Foremost, the *MDZ* approach does not incorporate certain factors that may influence a location's moisture supply at a finer spatial scale, such as winter snowpack, surface runoff, or groundwater storage. Furthermore, although the maps use a standardized index scale that applies regardless of the size of the time window, the window size may still deserve some consideration. For instance, an extreme drought that persists over a 5-year period has substantially different forest health implications than an extreme drought over a 1-year period. While the 1-year, 3-year, and 5-year *MDZ* maps may together provide a comprehensive short-term overview, it may also be important to consider a particular region's longer-term moisture history when assessing the current health of its forests. For example, in geographic regions where droughts have historically occurred on a frequent (e.g., annual or nearly annual) basis, certain tree species may be better adapted to a regular lack of available moisture (McDowell and others 2008). Because of this variability in species' drought tolerance, a long period of persistent and severe drought conditions could ultimately lead to changes in regional forest composition (Mueller and others 2005); compositional changes may similarly arise from a long period of persistent moisture surplus (McEwan and others 2011). In turn, such changes are likely to affect regional responses to future drought or surplus conditions, fire regimes, and the status of ecosystem services such as nutrient cycling and wildlife habitat (W.R.L. Anderegg and others 2013, DeSantis and others 2011). In future work, we hope to provide forest managers and other decision makers with better quantitative evidence regarding critical relationships between moisture extremes and significant forest health impacts such as regional-scale tree mortality (e.g., Mitchell and others 2014). We also intend to examine the capacity of moisture extremes to serve as inciting factors, and thus as predictors, for other forest threats such as wildfire or pest outbreaks. For example, Westerling and others (2003) asserted that the relationship between drought and wildfire in the Western United States is strong enough to support reliable prediction of regional fire season severity as much as a year in advance. Ultimately, our goal is to be able to make these types of forecasts at the national level.

LITERATURE CITED

Adams, D.K.; Comrie, A.C. 1997. The North American monsoon. Bulletin of the American Meteorological Society. 78(10): 2197–2213.

Adams, H.D.; Guardiola-Claramonte, M.; Barron-Gafford, G.A. [and others]. 2009. Temperature sensitivity of drought-induced tree mortality portends increased regional die-off under global-change-type drought. Proceedings of the National Academy of Sciences. 106(17): 7063–7066.

Akin, W.E. 1991. Global patterns: climate, vegetation, and soils. Norman, OK: University of Oklahoma Press. 370 p.

Allen, C.D.; Macalady, A.K.; Chenchouni, H. [and others]. 2010. A global overview of drought and heat-induced tree mortality reveals emerging climate change risks for forests. Forest Ecology and Management. 259(4): 660–684.

Alley, W.M. 1984. The Palmer Drought Severity Index: limitations and assumptions. Journal of Climate and Applied Meteorology. 23: 1100–1109.

Anderegg, L.D.L.; Anderegg, W.R.L.; Berry, J.A. 2013. Not all droughts are created equal: translating meteorological drought into woody plant mortality. Tree Physiology. 33(7): 672–683.

Anderegg, W.R.L.; Kane, J.M.; Anderegg, L.D.L. 2013. Consequences of widespread tree mortality triggered by drought and temperature stress. Nature Climate Change. 3(1): 30–36.

Archaux, F.; Wolters, V. 2006. Impact of summer drought on forest biodiversity: what do we know? Annals of Forest Science. 63: 645–652.

Berdanier, A.B.; Clark, J.S. 2016. Multiyear drought-induced morbidity preceding tree death in southeastern U.S. forests. Ecological Applications. 26(1): 17–23.

Boddy, J. 2016. As record Appalachian wildfires fizzle out, scientists look to learn from the destruction. ScienceInsider. December 21 2016. American Association for the Advancement of Science. http://www.sciencemag.org/news/2016/12/record-appalachian-wildfires-fizzle-out-scientists-look-learn-destruction. [Date accessed: August 2, 2017].

Clark, J.S. 1989. Effects of long-term water balances on fire regime, north-western Minnesota. Journal of Ecology. 77: 989–1004.

Cleland, D.T.; Freeouf, J.A.; Keys, J.E. [and others]. 2007. Ecological subregions: sections and subsections for the conterminous United States. Gen. Tech. Rep. WO-76D [Map; Sloan, A.M., cartographer; presentation scale 1:3,500,000; colored]. Washington, DC: U.S. Department of Agriculture, Forest Service. Also on CD-ROM as a GIS coverage in ArcINFO format or at http://data.fs.usda.gov/geodata/edw/datasets.php. [Date accessed: July 20, 2015].

Clinton, B.D.; Boring, L.R.; Swank, W.T. 1993. Canopy gap characteristics and drought influences in oak forests of the Coweeta Basin. Ecology. 74(5): 1551–1558.

Daly, C.; Gibson, W.P.; Taylor, G.H. [and others]. 2002. A knowledge-based approach to the statistical mapping of climate. Climate Research. 22: 99–113.

DeSantis, R.D.; Hallgren, S.W.; Stahle, D.W. 2011. Drought and fire suppression lead to rapid forest composition change in a forest-prairie ecotone. Forest Ecology and Management. 261(11): 1833–1840.

Duever, M J.; Meeder, J.F.; Meeder, L.C.; McCollum, J.M. 1994. The climate of south Florida and its role in shaping the Everglades ecosystem. In: Davis, S.M.; Ogden, J.C., eds. Everglades: the ecosystem and its restoration. Delray Beach, FL: St. Lucie Press: 225–248.

Elkinton, J.; Boettner, J. 2016. Gypsy moth outbreak of 2016. Massachusetts Wildlife Magazine No. 3, 2016. http://www.mass.gov/eea/agencies/dfg/dfw/publications/gypsy-moth-outbreak-of-2016.html. [Date accessed: August 2, 2017].

Grundstein, A. 2009. Evaluation of climate change over the continental United States using a moisture index. Climatic Change. 93: 103–115.

Guarín, A.; Taylor, A.H. 2005. Drought triggered tree mortality in mixed conifer forests in Yosemite National Park, California, USA. Forest Ecology and Management. 218: 229–244.

Guttman, N.B.; Quayle, R.G. 1996. A historical perspective of U.S. climate divisions. Bulletin of the American Meteorological Society. 77(2): 293–303.

Hanson, P.J.; Weltzin, J.F. 2000. Drought disturbance from climate change: response of United States forests. Science of the Total Environment. 262: 205–220.

Kareiva, P.M.; Kingsolver, J.G.; Huey, B.B., eds. 1993. Biotic interactions and global change. Sunderland, MA: Sinauer Associates, Inc. 559 p.

Keetch, J.J.; Byram, G.M. 1968. A drought index for forest fire control. Asheville, NC: U.S. Department of Agriculture, Forest Service, Southeastern Forest Experiment Station. 33 p.

Koch, F.H.; Coulston, J.W. 2015. 1-year (2013), 3-year (2011–2013), and 5-year (2009–2013) drought maps for the conterminous United States. In: Potter, K.M.; Conkling, B.L., eds. Forest Health Monitoring: national status, trends, and analysis 2014. Gen. Tech. Rep. SRS-209. Asheville, NC: US Department of Agriculture, Forest Service, Southern Research Station: 57–71.

Koch, F.H.; Coulston, J.W. 2016. 1-year (2014), 3-year (2012–2014), and 5-year (2010–2014) maps of drought and moisture surplus for the conterminous United States. In: Potter, K.M.; Conkling, B.L., eds. Forest Health Monitoring: national status, trends, and analysis 2015. Gen. Tech. Rep. SRS-213. Asheville, NC: US Department of Agriculture, Forest Service, Southern Research Station: 61–78.

Koch, F.H.; Coulston, J.W. 2017. Moisture deficit and surplus in the conterminous United States for three time windows: 2015, 2013–2015, and 2011–2015. In: Potter, K.M.; Conkling, B.L., eds. Forest Health Monitoring: national status, trends, and analysis 2016. Gen. Tech. Rep. SRS-222. Asheville, NC: US Department of Agriculture, Forest Service, Southern Research Station: 63–80.

Koch, F.H.; Coulston, J.W.; Smith, W.D. 2012a. High-resolution mapping of drought conditions. In: Potter, K.M.; Conkling, B.L., eds. Forest Health Monitoring 2008 national technical report. Gen. Tech. Rep. SRS-158. Asheville, NC: US Department of Agriculture, Forest Service, Southern Research Station: 45–62.

Koch, F.H.; Coulston, J.W.; Smith, W.D. 2012b. Mapping drought conditions using multi-year windows. In: Potter, K.M.; Conkling, B.L., eds. Forest Health Monitoring 2009 national technical report. Gen. Tech. Rep. SRS-167. Asheville, NC: US Department of Agriculture, Forest Service, Southern Research Station: 163–179.

Koch, F H.; Smith, W.D.; Coulston, J.W. 2013a. An improved method for standardized mapping of drought conditions. In: Potter, K.M.; Conkling, B.L., eds. Forest Health Monitoring: national status, trends, and analysis 2010. Gen. Tech. Rep. SRS-176. Asheville, NC: US Department of Agriculture, Forest Service, Southern Research Station: 67–83.

Koch, F.H.; Smith, W.D.; Coulston, J.W. 2013b. Recent drought conditions in the conterminous United States. In: Potter, K.M.; Conkling, B.L., eds. Forest Health Monitoring: national status, trends, and analysis 2011. Gen. Tech. Rep. SRS-185. Asheville, NC: US Department of Agriculture, Forest Service, Southern Research Station: 41–58.

Koch, F.H.; Smith, W.D.; Coulston, J.W. 2014. Drought patterns in the conterminous United States and Hawai'i. In: Potter, K.M.; Conkling, B.L., eds. Forest Health Monitoring: national status, trends, and analysis 2012. Gen. Tech. Rep. SRS-198. Asheville, NC: US Department of Agriculture, Forest Service, Southern Research Station: 49–72.

Koch, F.H.; Smith, W.D.; Coulston, J.W. 2015. Drought patterns in the conterminous United States, 2012. In: Potter, K.M.; Conkling, B.L., eds. Forest Health Monitoring: national status, trends, and analysis 2013. Gen. Tech. Rep. SRS-207. Asheville, NC: US Department of Agriculture, Forest Service, Southern Research Station: 55–69.

Kolb, T.E.; Fettig, C.J.; Ayres, M.P. [and others]. 2016. Observed and anticipated impacts of drought on forest insects and diseases in the United States. Forest Ecology and Management. 380: 321–334.

Laurance, S.G.W.; Laurance, W.F.; Nascimento, H.E.M. [and others]. 2009. Long-term variation in Amazon forest dynamics. Journal of Vegetation Science. 20(2): 323–333.

Luce, C.H.; Vose, J.M.; Pederson, N. [and others]. 2016. Contributing factors for drought in United States forest ecosystems under projected future climates and their uncertainty. Forest Ecology and Management. 380: 299–308.

Martínez-Vilalta, J.; Lloret, F.; Breshears, D.D. 2012. Drought-induced forest decline: causes, scope and implications. Biology Letters. 8(5): 689–691.

Mattson, W.J.; Haack, R.A. 1987. The role of drought in outbreaks of plant-eating insects. BioScience. 37(2): 110–118.

McDowell, N.; Pockman, W.T.; Allen, C.D. [and others]. 2008. Mechanisms of plant survival and mortality during drought: why do some plants survive while others succumb to drought? New Phytologist. 178: 719–739.

McEwan, R.W.; Dyer, J.M.; Pederson, N. 2011. Multiple interacting ecosystem drivers: toward an encompassing hypothesis of oak forest dynamics across eastern North America. Ecography. 34: 244–256.

McKee, T.B.; Doesken, N.J.; Kleist, J. 1993. The relationship of drought frequency and duration to time scales. In: Eighth Conference on Applied Climatology. Boston, MA: American Meteorological Society: 179–184.

Millar, C.I.; Westfall, R.D.; Delany, D.L. 2007. Response of high-elevation limber pine (*Pinus flexilis*) to multiyear droughts and 20th-century warming, Sierra Nevada, California, USA. Canadian Journal of Forest Research. 37: 2508–2520.

Mitchell, P.J.; O'Grady, A.P.; Hayes, K.R.; Pinkard, E.A. 2014. Exposure of trees to drought-induced die-off is defined by a common climatic threshold across different vegetation types. Ecology and Evolution. 4(7): 1088–1101.

Monteith, J.L. 1965. Evaporation and environment. Symposia of the Society for Experimental Biology. 19: 205–234.

Mueller, R.C.; Scudder, C.M.; Porter, M.E. [and others]. 2005. Differential tree mortality in response to severe drought: evidence for long-term vegetation shifts. Journal of Ecology. 93: 1085–1093.

Namias, J. 1966. Nature and possible causes of the northeastern United States drought during 1962–1965. Monthly Weather Review. 94(9): 543–554.

Namias, J. 1983. Some causes of United States drought. Journal of Climate and Applied Meteorology. 22: 30–39.

National Climatic Data Center. 2015. Divisional temperature-precipitation-drought. Documentation for the nClimDiv database. ftp://ftp.ncdc.noaa.gov/pub/data/cirs/climdiv/divisional-readme.txt. [Date accessed: July 29, 2015].

National Climatic Data Center. 2017a. Climatological rankings - temperature, precipitation, and drought. http://www.ncdc.noaa.gov/temp-and-precip/climatological-rankings/index.php. [Date accessed: August 3, 2017].

National Climatic Data Center. 2017b. State of the climate - drought - annual report 2016 [Web page]. https://www.ncdc.noaa.gov/sotc/drought/201613. [Date accessed: August 2, 2017].

Palmer, W.C. 1965. Metereological drought. Washington, DC: U.S. Department of Commerce, Weather Bureau. 58 p.

Peng, C.; Ma, Z.; Lei, X. [and others]. 2011. A drought-induced pervasive increase in tree mortality across Canada's boreal forests. Nature Climate Change. 1(9): 467–471.

Peters, M.P.; Iverson, L.R.; Matthews, S.N. 2015. Long-term droughtiness and drought tolerance of eastern U.S. forests over five decades. Forest Ecology and Management. 345: 56–64.

Potter, C.S.; Klooster, S.A. 1999. Dynamic global vegetation modelling for prediction of plant functional types and biogenic trace gas fluxes. Global Ecology and Biogeography. 8(6): 473–488.

PRISM Climate Group. 2017. 2.5-arcmin (4 km) gridded monthly climate data. http://www.prism.oregonstate.edu. [Date accessed: June 12, 2017].

Raffa, K.F.; Aukema, B.H.; Bentz, B.J. [and others]. 2008. Cross-scale drivers of natural disturbances prone to anthropogenic amplification: the dynamics of bark beetle eruptions. BioScience. 58(6): 501–517.

Rind, D.; Goldberg, R.; Hansen, J. [and others]. 1990. Potential evapotranspiration and the likelihood of future drought. Journal of Geophysical Research: Atmospheres. 95(D7): 9983–10004.

Rozas, V.; García-González, I. 2012. Too wet for oaks? Inter-tree competition and recent persistent wetness predispose oaks to rainfall-induced dieback in Atlantic rainy forest. Global and Planetary Change. 94–95: 62–71.

Rozas, V.; Sampedro, L. 2013. Soil chemical properties and dieback of *Quercus robur* in Atlantic wet forests after a weather extreme. Plant and Soil. 373(1–2): 673–685.

Schoennagel, T.; Veblen, T.T.; Romme, W.H. 2004. The interaction of fire, fuels, and climate across Rocky Mountain forests. BioScience. 54(7): 661–676.

Southeast Regional Climate Center. 2016. Quarterly climate impacts and outlook– regional weather pattern and highlights for Autumn 2016. http://www.sercc.com/Southeast_Region_Quarterly_Report_Autumn_2016.pdf. [Date accessed: August 2, 2017].

Steinemann, A. 2003. Drought indicators and triggers: a stochastic approach to evaluation. Journal of the American Water Resources Association. 39(5): 1217–1233.

Svoboda, M.; LeComte, D.; Hayes, M. [and others]. 2002. The Drought Monitor. Bulletin of the American Meteorological Society. 83(8): 1181–1190.

Teskey, R.; Wertin, T.; Bauweraerts, I. [and others]. 2015. Responses of tree species to heat waves and extreme heat events. Plant, Cell & Environment. 38(9): 1699–1712.

Thornthwaite, C.W. 1948. An approach towards a rational classification of climate. Geographical Review. 38(1): 55–94.

Thornthwaite, C.W.; Mather, J.R. 1955. The water balance. Publications in Climatology. 8(1): 1–104.

Trouet, V.; Taylor, A.H.; Wahl, E.R. [and others]. 2010. Fire-climate interactions in the American West since 1400 CE. Geophysical Research Letters. 37(4): L04702.

U.S. Department of Agriculture (USDA) Office of Communications. 2016. New aerial survey identifies more than 100 million dead trees in California. News Release No. 0246.16. http://www.usda.gov/wps/portal/usda/usdamediafb?contentid=2016/06/0150.xml. [Date accessed: August 7, 2017].

Westerling, A.L.; Gershunov, A.; Brown, T.J. [and others]. 2003. Climate and wildfire in the western United States. Bulletin of the American Meteorological Society. 84(5): 595–604.

Williams, A.P.; Allen, C.D.; Macalady, A.K. [and others]. 2013. Temperature as a potent driver of regional forest drought stress and tree mortality. Nature Climate Change. 3(3): 292–297.

Willmott, C.J.; Feddema, J.J. 1992. A more rational climatic moisture index. Professional Geographer. 44(1): 84–87.